Josephson Ladders

A. V. Ustinov

Physikalisches Institut III
Universität Erlangen-Nürnberg

This review is based on joint works with

D. Abraimov, P. Binder, P. Caputo, G. Filatrella, M.V. Fistul, S. Flach, B. A. Malomed, M. Schuster, and Y. Zolotaryuk.

- *P. Caputo et al. Phys. Rev. B **59**, 14050 (1999).*
- *D. Abraimov et al. Phys. Rev. Lett. **83**, 5354 (1999)*
- *P. Binder et al. Phys. Rev. Lett. **84**, 745 (2000)*
- *P. Binder et al. Phys. Rev. E **62**, 2858 (2000)*

See also at this conference:

Poster **P4YA1** by P. Binder et al.
Poster **P4SA1** by P. Caputo et al.

Outline

1. Josephson ladders: crossing over the border between 1D transmission lines and 2D arrays

2. Recalling underdamped parallel 1D arrays

3. Electromagnetic **wave propagation** in ladders

Pt.1
- experiment: IV curves in magnetic field
- resonances, dispersion relation
- dependence on the ladder anisotropy
- propagation of fluxons

4. Observation of **localized excitations** in ladders

Pt.2
- discrete breathers in nonlinear lattices
- our tool: low temperature laser microscope
- excitation of roto-breathers
- annular ladders
- open-boundary ladders
- symmetry of the observed states

5. Metastable localized states in larger systems: meandered row switching in 2D arrays

Summary of Pt.1:

Wave propagation in ladders

1. Linear electromagnetic waves lead to resonances that are observed on IV curves

2. These resonances are well explained by the dispersion relation (multiple branches)

3. Static properties: ladder vs 1D array
$$\beta^{eff}_{L} \rightarrow \beta_L + 2/\eta$$

4. Fluxon motion: locking to Josephson plasmons in both vertical and horizontal junctions

5. Ballistic fluxon propagation: strongly influenced by the anisotropy parameter $\eta = I_{CH}/I_{CV}$

Summary of Pt.2

Localized excitations in ladders

1. Discrete rotobreathers are directly visualized in Josephson ladders

2. Diversity of multi-site states is observed

3. Breather states are also found to occur spontaneously (with no local force)

4. Both the top-bottom symmetric and anti-symmetric states are found

5. To be studied: Stability range *vs.* damping, discreteness, and anisotropy; plasmon scattering on breathers

6. This is the first direct observation of discrete breathers in a nonlinear lattice

This publication is based (partly) on the presentations made at the European Research Conference (EURESCO) on "Future Perspectives of Superconducting Josephson Devices: Euroconference on Physics and Application of Multi-Junction Superconducting Josephson Devices, Acquafredda di Maratea, Italy, 1-6 July 2000, organised by the European Science Foundation and supported by the European Commission, Research DG, Human Potential Programme, High-Level Scientific Conferences, Contract HPCFCT-1999-00135. This information is the sole responsibility of the author(s) and does not reflect the ESF or Community's opinion. The ESF and the Community are not responsible for any use that might be made of data appearing in this publication."

Related works
(discrete breathers in Josephson ladders)

Theory of discrete breathers in Josephson ladders

- *L.M.Floria, J.L.Marin, P.J.Martinez, F.Falo, and S.Aubry*
  Europhys. Lett. ***36****, 539 (1996)*

- *S. Flach and M. Spicci*
  J. Phys. Cond. Matt. ***11****, 321 (1999)*

- *J. J. Mazo, E. Trias, and T. P. Orlando*
  Phys. Rev. B ***59****, 13604 (1999)*

Experiment of MIT group (1- and 2- site breathers)

- *E. Trias, J. J. Mazo, and T. P. Orlando,*
  Phys.Rev.Lett. 84, 741 (2000)

See also at this conference:

Poster **P4YA1** by P. Binder et al

Poster **P4YA4** by J. J. Mazo et al.

Cavity resonances in Josephson ladders

P. Caputo, M. V. Fistul, and A. V. Ustinov
Physikalisches Institut III, Universität Erlangen-Nürnberg, Erwin-Rommel-Strasse 1, D-91058 Erlangen, Germany

B. A. Malomed
Department of Interdisciplinary Studies, Faculty of Engineering, Tel Aviv University, Tel Aviv 59978, Israel

S. Flach
Max-Planck-Institut für Physik komplexer-Systeme, Vothnitzev Strasse 38, D-01187 Dresden, Germany
(Received 7 August 1998)

Electromagnetic waves which propagate along a Josephson junction ladder are shown to manifest themselves by resonant steps in the current-voltage characteristics. We report on experimental observation of resonances in ladders of different geometries. The step voltages are mapped on the wave dispersion relation which we derive analytically for the general case of a ladder of arbitrary anisotropy. Using the developed model, current amplitudes of the resonances are also calculated and their dependence on magnetic field is found to be in good accord with experiment. [S0163-1829(99)06121-4]

Josephson junction ladders have given rise to a great deal of interest in the past few years.[1–7] These quasi-one-dimensional (1D) structures are more complex than already well-understood 1D parallel Josephson junction arrays or long Josephson junctions. In contrast to the latter systems, a ladder contains small Josephson junctions in the direction transverse to the bias current (Fig. 1). The ladder can be viewed as the elementary row of a two-dimensional Josephson junction array which, in general, shows very complex dynamics. Thus, better understanding of electromagnetic properties of ladders may lead to new insight into the dynamics of underdamped 2D Josephson junction arrays.

For experimentally relevant modeling of Josephson ladders it is important to take into account magnetic field screening effects which are related to the finite inductances of elementary cells. Using the simplest model with only self-inductances taken into account, both static[2,3,6,7] and some of the dynamic[4–6] properties of ladders have been recently investigated. However, one of the basic characteristics of these systems such as the dispersion relation for small-amplitude waves remained unstudied until now. As in the case of long junctions and 1D parallel arrays, cavity resonances in underdamped ladders can be important as experimentally measurable ''fingerprints'' of their electrodynamic properties.

In this paper we report on the observation of cavity resonances in Josephson junction ladders with different anisotropy. We also derive the dispersion relation for linear waves in ladders which allows us to consistently explain the measurements and also interpret previously published data by other authors.

The measured ladders consist of Nb/Al-AlO_x/Nb underdamped Josephson tunnel junctions. We investigated both the annular geometry and the linear geometry ladders, sketched in Fig. 1. Each cell of a ladder contains four small junctions. The bias current $I_{\rm ext}$ is injected uniformly at every node via the external resistors. Here, we call *vertical* (JJ_V) the junctions placed in the direction of the external bias current, and *horizontal* (JJ_H) the junctions transverse to the bias. The ladder voltage is read across the vertical junctions.

We have measured current-voltage (I-V) characteristics of annular ladders with two different values of the ratio of the JJ_H's area S_H to JJ_V's area S_V. This ratio is referred in the following as anisotropy factor $\eta = I_{cH}/I_{cV}$, defined in terms of the junction critical currents. Our annular ladders have either $\eta = 0.5$ ($S_H = 16\ \mu\text{m}^2$, $S_V = 32\ \mu\text{m}^2$) or $\eta = 1$ ($S_H = S_V = 16\ \mu\text{m}^2$). The number of cells is $N = 12$, the cell size $A = 135\ \mu\text{m}^2$. The studied linear ladders have $\eta = 1$ ($S_H = S_V = 16\ \mu\text{m}^2$), $N = 15$, and $A = 140\ \mu\text{m}^2$. The discreteness of the ladder is expressed in terms of the parameter $\beta L = 2\pi I_{cV} L/\Phi_0$, where L is the self-inductance of the elementary cell of the ladder, I_{cV} is the critical current of the single vertical junction, and Φ_0 is the magnetic flux quantum. The cell inductance can be roughly estimated as L

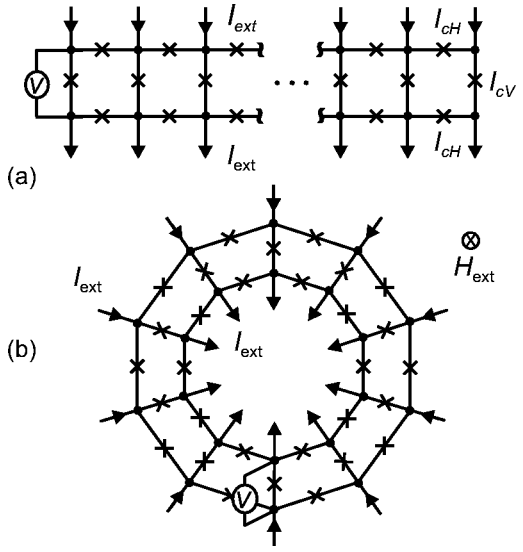

FIG. 1. Sketches of 1D Josephson junction ladders: (a) linear geometry; (b) annular geometry ($N = 10$).

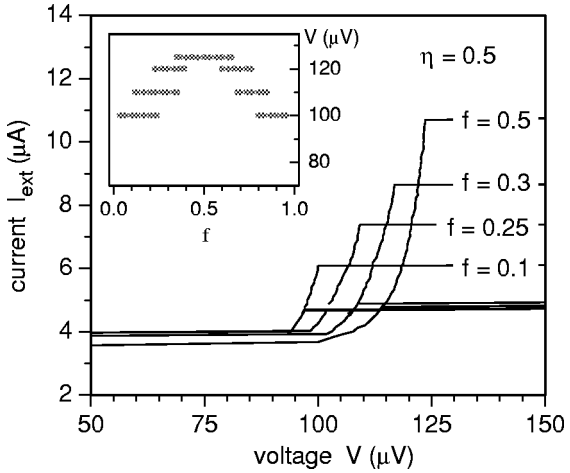

FIG. 2. Current-voltage characteristics of an annular Josephson ladder with anisotropy $\eta=0.5$ for different values of frustration f. Temperature $T=4.2$ K. Inset: Measured V_+ vs f at the same temperature; the horizontal branches indicate the step stability range.

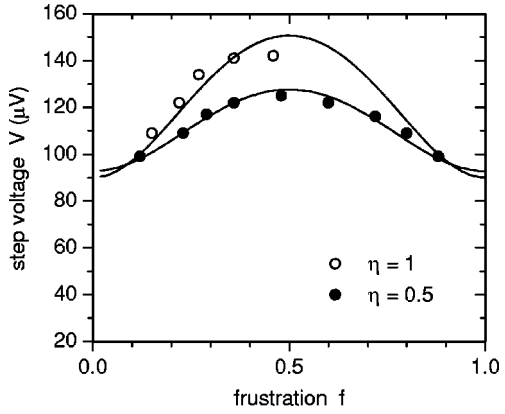

FIG. 3. Experimental (circles) and theoretical (solid lines) dependencies of the resonance voltages V_+ on the frustration f for two annular Josephson ladders. Results are shown for isotropic (open circles) and anisotropic (solid circles) ladders. Temperature $T\approx5.7$ K. To fit the experimental data by Eq. (3), we have used the parameters $\eta=1$ with $\beta=0.16$ and $\eta=0.5$ with $\beta=0.3$.

$=1.25\mu_0\sqrt{A}$, where μ_0 is the magnetic permeability. At $T=4.2$ K, the values of β are between 0.1 and 0.2, depending on the vertical junction critical current. The damping of the ladder is given in terms of the junction McCumber parameter, defined as $\beta_c=2\pi I_{cV,H}R^2_{V,H}C_{V,H}/\Phi_0$. Here $R_{V,H}$ is the subgap resistance; $C_{V,H}$ is the junction capacitance, calculated from the Fiske modes in a long junction on the same chip ($C/S=3.4$ μF/cm^2). At $T=4.2$ K, typical values of β_c for annular ladders are around 200. The applied field $H_{\rm ext}$ is transverse to the cells plane and is expressed in terms of the frustration f, defined as the magnetic flux threading the cell normalized to Φ_0.

In the presence of frustration, the I-V curves of the ladders show steps with resonant behavior. These steps occur at fixed voltage positions and are split in two voltage domains denoted by V_+ and V_- (upper and lower voltage resonances). Figure 2 shows an enlargement of the I-V curves of the anisotropic annular ladder in the voltage region where the upper resonances V_+ appear. The curves were recorded at different values of frustration for $T=4.2$ K. At this temperature, in both the anisotropic and isotropic annular ladders, only four resonances V_+ are present in the region of frustration $0\leqslant f\leqslant0.5$. A slight increase of the temperature leads to the appearance of the fifth resonance, at about $f=0.4$. Each step is located at a given voltage position and shows a resonant dependence of its magnitude on f (see the inset of Fig. 2). In contrast to 1D parallel arrays (no horizontal junctions, $\eta=\infty$), in ladders the reduction of the Josephson critical current due to frustration is rather small,[2] even in the case of low β. As a consequence of this, at any f the critical current of a ladder is always larger than the amplitude of the resonances, and the ladder switches from the zero voltage state directly to the gap voltage state. The only way to bias the ladder on one of the resonances is to follow the backward hysteretic branch of the I-V curve to the bottom part of the resonance. The voltage spacing between the higher steps is slightly reduced. Inversely, the current amplitude of the resonances increases with voltage, and the resonance at $f=0.5$ has the maximum height.

In both annular and linear ladders the voltage of the resonances is field dependent and approaches its maximum at $f=0.5$. We show these dependencies for isotropic and anisotropic annular ladders in Fig. 3 and for a linear ladder in Fig. 4. All curves are found to be nearly symmetric with respect to $f=0.5$. Thus, for the isotropic case we show data only up to $f=0.5$.

In Fig. 4 the two resonances V_+ and V_- for the linear ladder are compared with the resonant step in a linear 1D parallel array. The 1D array has the same number of cells and cell and junction areas as the ladder. A small difference in their critical currents gives $\beta=0.12$ for the ladder, and $\beta=0.17$ for the array. The responses of the ladder and 1D array to the frustration are very different. In the 1D array, there is only one resonance (V_{PA}), and the voltage of this resonance follows the well known sin-like dependence on f. Above a critical value of frustration ($f\approx0.1$) the resonance appears, by increasing f it moves to higher voltages, and at $f=0.5$ it saturates at the value $V_{PA}=135$ μV. The ladders, instead, have two branches V_- and V_+, which are confined in two different voltage regions. Both V_- and V_+ have the same f periodicity as V_{PA}. In contrast to the annular case, in

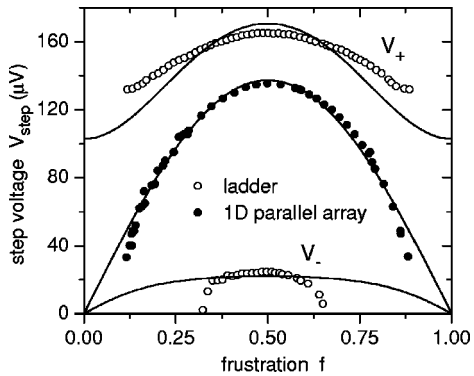

FIG. 4. Experimental (circles) and theoretical (lines) dependencies of the voltage position of two resonances $V_\pm(f)$ on the frustration for the linear isotropic ladder. The dependence of the resonance voltage position on the frustration for the parallel array ($\eta=\infty$) is also shown (solid circles).

the linear ladders V_- and V_+ were found to be continuously tuned by field in the ranges $0 \leqslant V_- \leqslant 25\ \mu$V and $135 \leqslant V_+ \leqslant 165\ \mu$V, respectively.

In the following, we present a theory of I-V resonances for a Josephson junction ladder. The theory allows us to predict the voltages and the current magnitudes of resonances observed in experiment.

We use the time-dependent Josephson phases of vertical φ_n and horizontal $\psi_{n1,2}$ junctions. The indices 1 and 2 refer to the lower and upper branches of horizontal junctions, and n is the index of the cell in the ladder. For the upper and lower horizontal junctions we use the symmetry condition that $\psi_{n1} = -\psi_{n2} = \psi_n$.[2,5,8] According to the derivation done in Refs. 2,8 for the isotropic case, we use the resistively shunted model for Josephson junctions and the usual analysis for superconductive loops with only self-inductances taken into account to derive a set of normalized dynamical equations for the phases φ_n and ψ_n for the anisotropic case

$$\ddot{\varphi}_n + \alpha\dot{\varphi}_n + \sin\varphi_n = \frac{1}{\beta}[2\psi_n - 2\psi_{n-1} + \varphi_{n-1} - 2\varphi_n + \varphi_{n+1}] + \gamma\ ,$$

$$\ddot{\psi}_n + \alpha\dot{\psi}_n + \sin\psi_n = \frac{1}{\eta\beta}[\varphi_n - \varphi_{n+1} - 2\psi_n] + \frac{2\pi f}{\eta\beta},$$

$$n = 1, \ldots, N. \quad (1)$$

Here, the unit of time is $\omega_p^{-1} = \sqrt{\hbar C_V/(2eI_{cV})}$, the inverse of plasma frequency of the ladder. The parameter $\alpha = 1/\sqrt{\beta_c}$ determines the damping in the ladder. We have used the fact that the anisotropy in typical Josephson circuits is realized by choosing different areas of horizontal and vertical junctions. Thus, the condition $I_{cH}/I_{cV} = C_H/C_V = R_V/R_H$ is assumed in Eq. (1). Note that, in this case, ω_p and α do not depend on anisotropy of the ladder. Finally, $\gamma = I_{\rm ext}/I_{cV}$ is the normalized bias current. In the finite voltage state we impose a whirling solution along the vertical junctions and oscillations with a small amplitude for the horizontal junctions.[9] Moreover, the phase of vertical junctions increases from cell to cell due to the presence of frustration. In this case, we quite naturally decompose the Josephson phases as follows:

$$\varphi_n = \omega t + 2\pi f n + \varphi e^{i(\omega t + 2\pi q n)},$$

$$\psi_n = \psi e^{i(\omega t + 2\pi q n)}, \quad (2)$$

where ω and q are the angular frequency and the wave number of the electromagnetic wave in the ladder. The time average Josephson current of vertical junctions is zero for this kind of a solution. In the limit of small amplitudes φ and ψ, we obtain the spectrum of electromagnetic wave propagating along the ladder. This spectrum consists of two branches $\omega_\pm(q)$ and is given by (in the usual units)

$$\omega_\pm = \omega_p\sqrt{F \pm \sqrt{F^2 - G}}, \quad (3)$$

where $F = \frac{1}{2} + 1/(\eta\beta) + (2/\beta)\sin^2(\pi q)$, and $G = (4/\beta)\sin^2(\pi q)$. This equation generalizes, for the case of the arbitrary wave number, the dynamical checkerboard state ($q = 0.5$) considered in Ref. 5. The presence of the horizontal junctions leads to two branches in the spectrum of electromagnetic waves. Moreover, the maximum value of ω_+ is higher than that of 1D parallel array and the dependence $\omega_+(q)$ is more flat.[10]

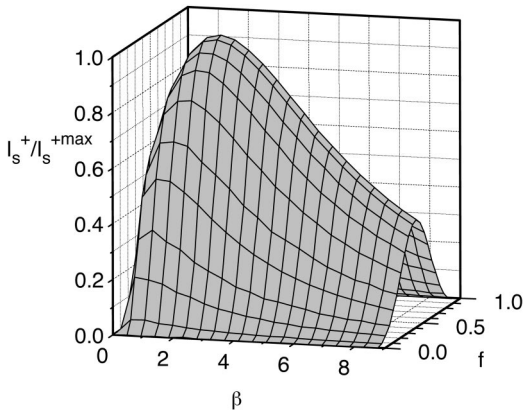

FIG. 5. Dependence of the maximum magnitude I_s^+ of the resonance V_+ on the self-inductance parameter β and frustration f for the isotropic ladder.

Note, that in the case of another particular ground state ($\langle\varphi_n\rangle = \langle\psi_n\rangle = 0$) instead of Eq. (2), the spectrum (3) is substituted by $\omega_+ = \omega_p\sqrt{2F}$ and $\omega_- = \omega_p$. This dispersion relation is important, e.g., for understanding the radiation by fluxon moving in the ladder.

As is well known, the electromagnetic waves interact with the oscillating Josephson current and this effect leads to the resonances on the I-V curve.[11,12] More precisely, the resonance conditions are

$$q_0 = f, \quad V_\pm = \frac{\hbar\omega_\pm(q_0)}{2e}. \quad (4)$$

The possibility to observe these resonances on the I-V curve depends on their current amplitudes. In the same limit of small amplitudes of the Josephson phases φ and ψ and by making use of the method elaborated in Refs. 11,12, the magnitudes of the resonances are given by

$$I_s^\pm = NI_{cV}\frac{1}{\alpha}\frac{\pm\sqrt{F^2 - G} - F + G}{\sqrt{F \pm \sqrt{F^2 - G}}\sqrt{F^2 - G}}. \quad (5)$$

The important result of this theory is that the amplitude of the resonance I_s^+ is small in the limits of both small and large β (see Fig. 5). Moreover, it has a maximum at $f = 0.5$. In the limit of very anisotropic ladder, when $\eta = \infty$, the magnitude of I_s^- of the resonance V_- decreases as $1/\eta$ and only the resonance V_+ can be observed. This is consistent with the case of 1D parallel arrays.

Using the developed theory, we can explain all important features of experimentally observed resonances on the current-voltage characteristic of Josephson ladders. First, due to the annular geometry only the electromagnetic waves with quantized wave numbers $q_n = n/N$ can propagate in the ladder. Here $n = 1, 2, \ldots, N$ is an integer. The resonances of

sufficiently large magnitude are observed on the I-V curve when the value of frustration matches these wave numbers [see Eq. (4)].

The experimentally observed dependence of the voltage V_+ on the frustration f, shown in Fig. 3, is well described by Eq. (3) for both isotropic and anisotropic annular ladders. We obtain a good quantitative agreement between theory and experiment using the plasma frequency $f=\omega_p/2\pi=14$ GHz (independent measurements give the value of $\omega_p \approx 16$ GHz) and the self-inductance parameters $\beta=0.16$ and 0.3, correspondingly, for isotropic and anisotropic cases. We also observe that the current magnitude of the resonances monotonically decreases when the frustration f deviates from the value 0.5 (see Fig. 2). It qualitatively agrees with the Eq. (5) for the maximum magnitude of the resonance.

In the case of annular ladder with $N=12$ cells, we may expect to observe six resonances in the region of $0 \leqslant f \leqslant 0.5$. In fact, we have observed only four stable resonances corresponding to the values of $n=2, 3, 4, 6$ (see Fig. 2). The resonance corresponding to the value of frustration $f=1/12$ is, apparently, not stable due to its small current magnitude as described by Eq. (5). Another resonance corresponding to the frustration $f=5/12$ is not stable at $T=4.2$ K, but we observed it at slightly higher temperature. The poor stability of this resonance can be due to its small distance from the neighboring resonance at $f \approx 1/2$.

Similar results have been obtained for Josephson junction ladder of linear geometry. We have observed two resonances V_+ and V_- in the upper and lower voltage regions. However, in this case, most probably due to a relatively low value of the subgap resistance (larger α) we have found that the dependence of their voltages on frustration is continuous (Fig. 4). Again, the resonance V_+ disappears in the limit of small frustration due to its small amplitude according to Eq. (5).

Finally, we have observed that the dependence $V_-(f)$ deviates from the theory [Eqs. (3) and (4)] in the region of frustration $f \leqslant 0.3$. This can be connected with the particular assumption on the state of the horizontal junctions. Our analysis has been carried out for the most simple state ($\langle \psi_n \rangle = 0$), but in general one might consider the case when the phases of the horizontal junctions undergo small amplitude oscillations around a finite angle. In this case, the resonance condition on the wave number q is not simply $q_0=f$, but a more complicated relationship can appear (see Ref. 9). The theoretical and experimental study of the properties of such general state, i.e., of the current-voltage characteristics of Josephson ladder in the region of small voltage, is in progress.

We thank H. Kohlstedt for providing us access to technological facilities for sample preparation at Forschungszentrum Jülich. P.C. and M.V.F. thank, respectively, the European Office of Aerospace Research and Development (EOARD) and the Alexander von Humboldt Stiftung for supporting this work.

[1] S. Ryu, W. Yu, and D. Stroud, Phys. Rev. E **53**, 2190 (1996).

[2] G. Grimaldi, G. Filatrella, S. Pace, and U. Gambardella, Phys. Lett. A **223**, 463 (1996).

[3] J. J. Mazo and J. C. Ciria, Phys. Rev. B **54**, 16 068 (1996).

[4] L. M. Floría, J. L. Martin, P. L. Martínez, F. Falo, and S. Aubry, Europhys. Lett. **36**, 539 (1996).

[5] M. Barahona, E. Trías, T. P. Orlando, A. E. Duwel, H. S. J. van der Zant, S. Watanabe, and S. H. Strogatz, Phys. Rev. B **55**, 11 989 (1997).

[6] E. Trías, M. Barahona, T. P. Orlando, and H. S. J. van der Zant, IEEE Trans. Appl. Supercond. **7**, 3103 (1997).

[7] M. Barahona, S. H. Strogatz, and T. P. Orlando, Phys. Rev. B **57**, 1181 (1998).

[8] G. Filatrella and K. Wiesenfeld, J. Appl. Phys. **78**, 1878 (1995).

[9] Equations (1) allow us to obtain a more general solution when the Josephson phase of the horizontal junctions $\psi_n=\psi_0+\psi e^{i(\omega t+2\pi q n)}$. The value of ψ_0 can be obtained as a solution of the transcendental equation $2\psi_0+\beta\eta \sin\psi_0=2\pi(f-q)$. In this case we have to use $\beta\cos\psi_0$ instead of β in Eqs. (3) and (5). However, for the ladder with $\beta \leqslant 1$ this solution is less stable than the one considered here [Eq. (2)].

[10] A. V. Ustinov, M. Cirillo, and B. A. Malomed, Phys. Rev. B **47**, 8357 (1993).

[11] I. O. Kulik, Zh. Tekh. Fiz. **37**, 157 (1967) [Sov. Phys. Tech. Phys. **12**, 111 (1967)].

[12] A. Barone and G. Paternó, *Physics and Applications of the Josephson Effect* (Wiley, New York, 1982).

Broken Symmetry of Row Switching in 2D Josephson Junction Arrays

D. Abraimov, P. Caputo, G. Filatrella,* M. V. Fistul, G. Yu. Logvenov,† and A. V. Ustinov
Physikalisches Institut III, Universität Erlangen-Nürnberg, D-91058 Erlangen, Germany
(Received 30 April 1999)

We present an experimental and theoretical study of row switching in two-dimensional Josephson junction arrays. We have observed novel dynamic states with peculiar percolative patterns of the voltage drop inside the arrays. These states were directly visualized using laser scanning microscopy and manifested by fine branching in the current-voltage characteristics of the arrays. Numerical simulations show that such percolative patterns have an intrinsic origin and occur independently of positional disorder. We argue that the appearance of these dynamic states is due to the presence of various metastable superconducting states in arrays.

PACS numbers: 74.50.+r, 47.54.+r, 74.80.–g

Spatiotemporal pattern formation in a system of nonlinear oscillators is governed by mutual coupling. Examples of such patterns are domain walls and kinks in arrays of coupled pendula, topological spin, and charge excitations in large molecules and solids, and inhomogeneous states in many other complex systems [1]. A single driven and damped nonlinear oscillator displays two distinctly different states, a static state and a whirling (dynamic) state. Therefore, a system of coupled oscillators can show various spatiotemporal patterns with concurrently present static and dynamic states.

Arrays of Josephson junctions have attracted a lot of interest because they serve as well-controlled laboratory objects to study such fundamental problems as above mentioned pattern formation, chaos, and phase locking. In the systems of coupled Josephson junctions [2–8] the two local states are the superconducting (static) state and the resistive (dynamic) state. For underdamped junctions, these states manifest themselves by various branches on the current-voltage (I-V) characteristics. The hysteretic switching between branches has been found in stacks of Josephson tunnel junctions [4], layered high temperature superconductors [5], and two-dimensional (2D) Josephson junction arrays [2,3,7,8].

In 2D arrays, this switching effect appears in the form of *row switching* when a voltage drop in the array occurs on individual rows of junctions perpendicular to the direction of the bias current. A typical behavior found in both experiments [7] and in numerical simulations [3,9] is that the number of rows switched to a resistive state and, even more important, their distribution inside the array can change during sweeping the I-V curve. An analysis of such row switching has been carried out recently [8] to predict the range of stability of the various resistive states. However, until now only relatively simple resistive states have been found. These states correspond to a whirling state of *vertical* junctions (placed in the direction of the bias current) and small oscillations of the Josephson phase difference of *horizontal* junctions (transverse to the bias) around their equilibrium state [8].

In this Letter, we report on the observation of new dynamic states with peculiar percolative patterns of the voltage drop inside *homogeneously* biased arrays. We have found broken symmetry in row switching such that the dc voltage drop meanders between rows. These states appear in dc measurements in the form of fine branching on the I-V curves. The states have been visualized by using the low temperature scanning laser microscopy (LTSLM) [10]. We have also carried out numerical simulations in which similar dynamic states are found. The measured two-dimensional arrays consist of underdamped Nb/Al-AlO_x/Nb Josephson junctions [11]. The junctions are placed at the crossing of the superconducting striplines that are arranged in either the square lattice (with four junctions per elementary cell) or the triangular lattice (with three junctions per elementary cell). An optical image of a 2D square array and the equivalent electrical circuit are shown in Fig. 1. The junction area is 9 μm^2 and their critical current density is about 1.1 kA/cm^2 for the square array, and 0.1 kA/cm^2 for the triangular array, with a typical spread of junction parameters of about 5%. The square arrays consist of ten columns by ten rows and have the cell area $S = 38\ \mu\text{m}^2$. The triangular arrays are made of twelve columns by twelve rows and have $S = 160\ \mu\text{m}^2$. All arrays are underdamped and typical values of the McCumber parameter [12] β_c at $T = 4.2$ K are around 200. The parameter β_L characterizing the influence of self-inductance [6,8] changes from $\beta_L \simeq 0.5$ for triangular arrays to $\beta_L \simeq 2$ for square arrays.

The bias current I is injected uniformly via external resistors. The voltage is read in the direction along the bias, both across the whole array and across several individual rows. The I-V curves are digitally stored while sweeping of the bias current occurs. The I-V characteristic of the square array is shown in Fig. 2. For every bias polarity, the number of branches is equal to the number of rows which are at the gap voltage state $V_g \simeq 2.7$ mV, and the highest gap voltage corresponds to the sum of gap voltages of the ten rows. By choosing a bias point at a certain gap voltage, we can select the number of rows which

 0031-9007/99/83(25)/5354(4)$15.00

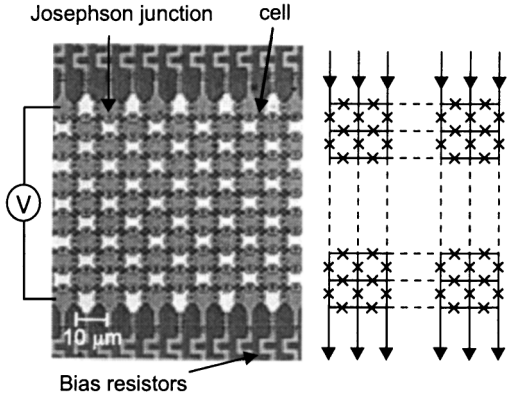

FIG. 1. Optical image and sketch of a 10×10 square array.

will be in the resistive state, while the other rows remain in the superconducting state.

On the hysteretic part of the I-V curves, we have systematically observed a fine branching around the row gap voltages [Fig. 3(a)]. The branching has been detected simply by recording a large number of I-V curves in the absence of externally applied magnetic field and at a constant sweep frequency and temperature ($T = 4.2$ K). It was always possible to choose a stable dc bias point on a particular branch. The fine branching of the I-V curves around the gap voltages was found to be a typical feature of all studied arrays.

In order to determine the actual distribution of resistive paths in the array, we used the method of LTSLM [10]. The LTSLM uses a focused laser beam for local heating of the sample. The local heating leads to an additional dissipation in the area of several micrometers in diameter. The laser beam induced variation of the voltage drop across the whole sample is recorded versus the beam coordinates. This method allows one to visualize the junctions that are in the resistive state. In order to increase the sensitivity and spatial resolution, the intensity of the beam is modulated at a frequency of several KHz and the voltage response of the array is the detected phase sensitively by a lock-in technique.

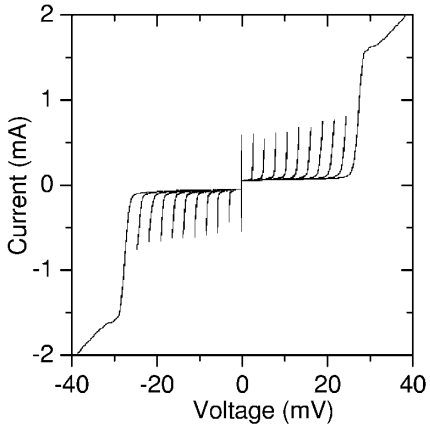

FIG. 2. Current-voltage characteristics of a 10×10 array.

By using the LTSLM, we have systematically imaged different resistive configurations biased at various fine resistive branches of the I-V curves. The experimental procedure is the following: the number n of switched rows is fixed by biasing the array at voltages $V \simeq nV_g$. Then LTSLM images of the sample are recorded at a constant bias current value. Typical images from the square array are shown in Figs. 3(b)–3(e). The black spots correspond to the junctions that are in the resistive state. The junctions that are in the superconducting state do not appear on the array image. As expected, the images show that the number of rows which are in the resistive state is equal to the number n of gap voltages selected by the bias point. To trap a different resistive configuration, we always increased the bias current I above I_c^{array}, the array critical current, and then reduced it to the low level.

Similarly to the experimental results of Ref. [7], we have found that most of the images show various combinations of *straight* resistive and superconducting rows [Figs. 3(b) and 3(c)]. However, the most striking feature of our measurements is that the resistive lines are not always straight, but may undergo a *meandering* towards the

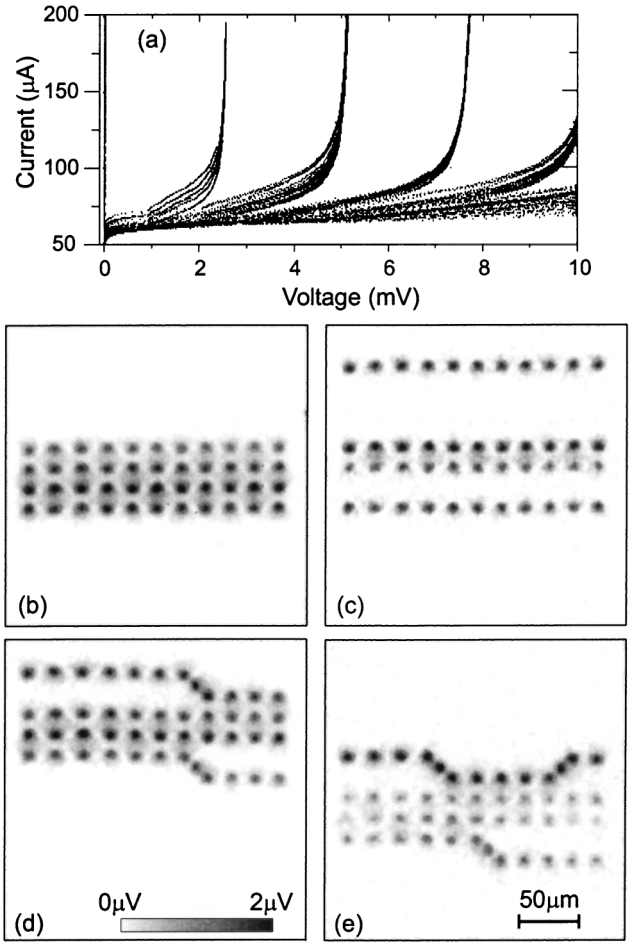

FIG. 3. (a) Enlargement of digitally stored I-V curves in the region between zero and $4V_g$; (b)–(e) LTSLM images of resistive states of the array at the bias points close to the $4V_g$.

neighboring row involving one of the horizontal junctions in the resistive state; see Fig. 3(d).

We have found that such a broken symmetry of row switching systematically appears in all studied arrays. Moreover, we have observed that the horizontal junctions switched to the resistive state were distributed randomly inside the array and have found no tendency for the meanders to occur at the same places. Thus, we suppose that the meandering is not predominantly due to any disorder in the junction parameters. The meandering of resistive paths is a rare event and its probability does not exceed 1% per horizontal junction of a single switched row. Therefore, the observation of deviation of resistive paths from the straight lines is easier for larger arrays. We have also observed rare resistive states with two switched horizontal junctions in one row, as shown in Fig. 3(e). Sometimes even more complicated distributions of switched junctions were registered [Figs. 4(a) and 4(b)].

In the following, we present numerical simulations of the dynamics of underdamped arrays. Calculations were performed using the resistively shunted model for Josephson junctions and the usual analysis for superconductive loops with only self-inductances taken into account, i.e., the Nakajima-Sawada equations [13]. For a discussion of these equations and the application limits see Refs. [6,8]. The phase configuration of a row switched state was used as the initial condition for the next run.

We simulated large (10×10) and small (2×10) square arrays with various parameter β_L between 0.5 and 2. In all cases, the simulations well reproduce the branching of I-V curves and the meandering character of the finite voltage paths. Moreover, in order to check the influence of self-inductance effects the simulation was carried out for the arrays with a small parameter $\beta_L = 0.1$. A simulated I-V curve with three different branches and the corresponding voltage distributions for the 2×10 array are shown in Fig. 5. Resistive states with both single and double meanders have been trapped (Fig. 5). The appearance of the meandering is qualitatively similar to the experimental images shown in Figs. 3(b)–3(e). The simulations have been carried out in the presence of a finite magnetic field in order to prevent the simultaneous switching of all the array rows [8]. It leads to the decrease of the critical current and the appearance of the flux-flow region where I-V curves are highly nonlinear (Fig. 5).

We have found that, in the absence of disorder, the probability of the appearance of a meander in two row array is about 1.8% per horizontal junction. Surprisingly, in the presence of specially introduced disorder up to 20% the numerical simulations show no increase of the rate of appearance and no preferred position of the meanders. Because of this fact, we conclude that the broken symmetry row switching appears due to an intrinsic instability of the superconducting state, i.e., a change of the initial conditions can lead to the appearance of a different percolative voltage path. The numerical analysis of the two row array also allows one to find out some peculiarities of the new dynamic states. When the junctions switched to the resistive state form a straight line in the top or bottom row (no meandering), the array has the highest resistance, $R_n/(N + 1)$ (triangle symbols in Fig. 5), where N is the total number of cells in the row and R_n is the normal resistance of one junction. In the case when the voltage path with one meandering occurs, the array shows a lower resistance, $R_n/(N + 2)$ (square, Fig. 5). Now there is one more junction connected in parallel to the resistive path, with respect to the case of no meandering. For the same reason, the meanders across two horizontal junctions correspond to the resistance $R_n/(N + 3)$ (circle, Fig. 5). The presence of meanders shifts the array I-V curve to the left and this resistance scaling explains the experimentally observed fine branching of the I-V curves.

These dynamic states are stable in a wide range of voltages, i.e., we have not observed direct switching between branches. This is due to the too large energy necessary for the junction capacitance recharge in underdamped arrays [12]. So, only switching from the superconducting state allows one to trap these dynamic states.

Our analysis using the Kirchhoff's current laws shows that, in the case of meandering, the dc superconducting current flows via the horizontal junctions. Moreover, this

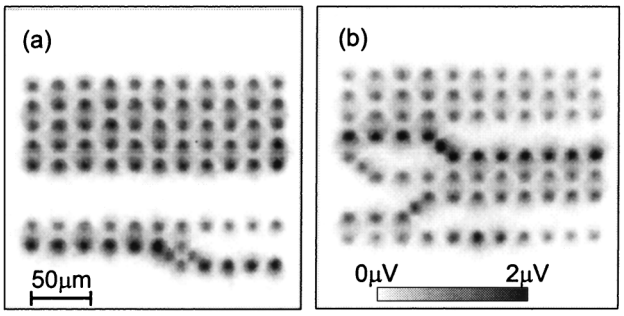

FIG. 4. LTSLM images of more complicated dynamic states observed at the bias points close to the $7V_g$ voltage region.

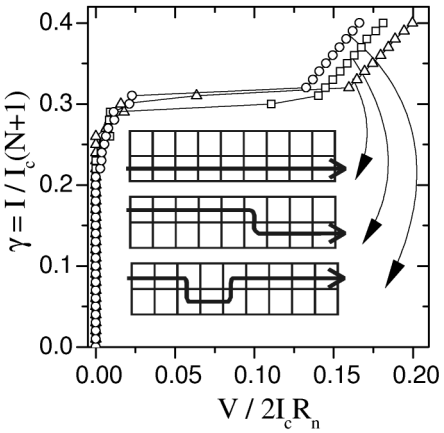

FIG. 5. Numerically simulated I-V characteristics of a two row array and the corresponding voltage paths at $\gamma = 0.4$. I_c is the single junction critical current.

current increases from the row boundary to the cell where the meandering occurs. This current configuration is different from that without meanders. In the latter case the horizontal junctions are not active and dc superconducting current flows only via the vertical junctions.

All these features can be explained, at least qualitatively, by the presence of metastable superconducting states in 2D Josephson arrays. We analyze these states for a simple case of two plaquettes with five junctions (Fig. 6). In the absence of the magnetic field, the most stable superconducting state is the one with all mesh currents equal to zero. At the bias current $I = 2I_c$ the vertical junctions switch from a superconducting state to a resistive state with straight resistive rows (dc mesh currents are still zero) [Fig. 6(a)]. However, this system has another peculiar state with finite values of mesh currents, as shown in Fig. 6(b). At $I = I_c$ this system can support a superconducting state with the Josephson phases of the horizontal junction and one vertical junction per row being equal to $\pi/2$. The Josephson phases of the remaining vertical junctions are equal to π. This metastable state supports finite mesh currents $I_c/2$ and switches to the dynamic (resistive) state with a meander via the horizontal junction. The mesh currents decrease to the value of $I_c/6$ and change sign during the switching process, which results in a stable dynamic state with meandering. Thus, the dynamic states with meandered dc voltage drop are "fingerprints" of metastable superconducting states with nonzero mesh currents and active horizontal junctions. The state appears only when there are at least three junctions per cell and it exists also in the limit of zero linear self-inductance and zero magnetic field [14]. That is different from the case of single- and double-junction SQUIDs, where metastable superconducting states appear only in the limit of large self-inductance [12]. Since the above discussed metastable state exists in the limit of zero inductance, the small arrays with few plaquettes can be a suitable system to observe the effect of macroscopic quantum coherence at low temperatures [12,15].

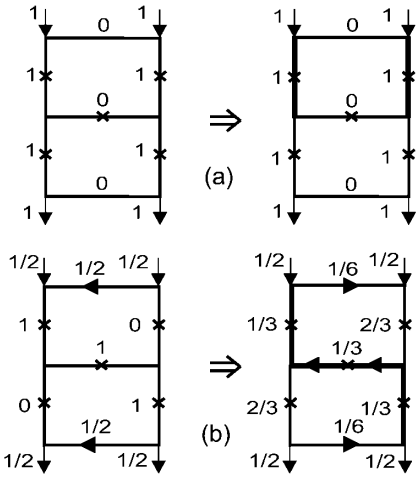

FIG. 6. Sketches of metastable superconducting and resistive states for a small array with two plaquettes containing three junctions per cell: (a) mesh currents are equal to zero; (b) mesh currents are different from zero. Thick solid lines show the parts of the array switched to resistive states, and the numbers are the local dc currents normalized to I_c.

It appears that also large 2D arrays can provide various metastable superconducting states that lead to the broken symmetry in the row switching process. Theoretical and experimental investigation of these metastable superconducting states and their dependence on the externally applied magnetic field are in progress.

This work was partially supported by the European Office of Aerospace Research and Development (EOARD), the Alexander von Humboldt Stiftung, the German-Israeli Foundation, and the German-Italian DAAD/Vigoni exchange program.

*Present address: Unitá INFM Salerno and Science Faculty, University of Sannio Via Port'Arsa 11, 82100 Benevento, Italy.

†Present address: OXXEL GmbH, Technologiepark Universität, Fahrenheitstrasse 9, D-28359 Bremen, Germany.

[1] S. H. Strogatz, *Nonlinear Dynamics and Chaos: With Applications to Physics, Biology, Chemistry, and Engineering* (Addison-Wesley, Reading, MA, 1994).

[2] H. S. J. van der Zant, C. J. Müller, L. J. Geerligs, C. J. P. M. Harmans, and J. E. Mooij, Phys. Rev. B **38**, 5154 (1988).

[3] W. Yu, K. H. Lee, and D. Stroud, Phys. Rev. B **47**, 5906 (1993).

[4] N. Thyssen, A. V. Ustinov, and H. Kohlstedt, J. Low. Temp. Phys. **106**, 201 (1997).

[5] R. Kleiner and P. Müller, Phys. Rev. B **49**, 1327 (1994).

[6] G. Filatrella and K. Wiesenfeld, J. Appl. Phys. **78**, 1878 (1995).

[7] S. G. Lachenmann, T. Doderer, D. Hoffmann, R. P. Hüebener, P. A. A. Booi, and S. P. Benz, Phys. Rev. B **50**, 3158 (1994).

[8] M. Barahona and S. Watanabe, Phys. Rev. B **57**, 10 893 (1998).

[9] J. R. Phillips, H. S. J. van der Zant, and T. P. Orlando, Phys. Rev. B **50**, 9380 (1994).

[10] A. G. Sivakov, A. P. Zhuravel', O. G. Turutanov, and I. M. Dmitrenko, Appl. Surf. Sci. **106**, 390 (1996).

[11] HYPRES Inc., Elmsford, NY 10523.

[12] K. K. Likharev, *Dynamics of Josephson Junctions and Circuits* (Gordon and Breach, New York, 1981).

[13] K. Nakajima and Y. Sawada, J. Appl. Phys. **52**, 5732 (1981).

[14] A similar state can be found in a single anisotropic plaquette with three junctions per cell when the parameter of anisotropy $\eta = I_{ch}/I_{cv} > 1/(2\sqrt{2})$ [M. V. Fistul (to be published)]. Here, I_{ch} and I_{cv} are, respectively, the critical currents of the horizontal and vertical junctions.

[15] J. E. Moiij, T. P. Orlando, L. Levitov, L. Tian, C. H. van der Wal, and S. Lloyd, Science **285**, 1036 (1999).

Observation of Breathers in Josephson Ladders

P. Binder,[1] D. Abraimov,[1] A. V. Ustinov,[1] S. Flach,[2] and Y. Zolotaryuk[2]
[1]*Physikalisches Institut III, Universität Erlangen, E.-Rommel-Straße 1, D-91058 Erlangen, Germany*
[2]*Max-Planck-Institut für Physik komplexer Systeme, Nöthnitzer Straße 38, D-01187 Dresden, Germany*
(Received 7 May 1999)

We report on the observation of spatially localized excitations in a ladder of small Josephson junctions. The excitations are whirling states which persist under a spatially homogeneous force due to the bias current. These states of the ladder are visualized using a low temperature scanning laser microscopy. We also compute breather solutions with high accuracy in corresponding model equations. The stability analysis of these solutions is used to interpret the measured patterns in the I-V characteristics.

PACS numbers: 74.50.+r, 05.45.Yv, 63.20.Ry

The present decade has been marked by an intense theoretical research on dynamical localization phenomena in spatially discrete systems, namely on discrete breathers (DB). These exact solutions of the underlying equations of motion are characterized by periodicity in time and localization in space. Away from the DB center the system approaches a stable (typically static) equilibrium. (For reviews, see [1,2]). These solutions are robust to changes of the equations of motion, and exist in translationally invariant systems and any lattice dimension. DBs have been discussed in connection with a variety of physical systems such as large molecules, molecular crystals [3], and spin lattices [4,5].

For a localized excitation such as a DB, the excitation of plane waves which might carry the energy away from the DB does not occur due to the spatial discreteness of the system. The discreteness provides a cutoff for the wavelength of plane waves and thus allows one to avoid resonances of all temporal DB harmonics with the plane waves. The nonlinearity of the equations of motion is needed to allow for the tuning of the DB frequency [1].

Though the DB concept was initially developed for conservative systems, it can be easily extended to dissipative systems [6]. There, discrete DBs become time-periodic spatially localized attractors, competing with other (perhaps nonlocal) attractors in phase space. The characteristic property of DBs in dissipative systems is that these *localized excitations* are predicted to persist under the influence of a *spatially homogeneous* driving force. This is due to the fact that the driving force compensates the dissipative losses of the DB.

So far, research in this field was predominantly theoretical. Identifying and analyzing of experimental systems for the direct observation of DBs thus becomes a very actual and challenging problem. Experiments on localization of light propagating in weakly coupled optical waveguides [7], low-dimensional crystals [8], and anti-ferromagnetic materials [9] have been recently reported.

In this work we realize the theoretical proposal [10] to observe DB-like localized excitations in arrays of coupled Josephson junctions. A Josephson junction is formed between two superconducting islands. Each island is characterized by a macroscopic wave function $\Psi \sim e^{i\theta}$ of the superconducting state. The dynamics of the junction is described by the time evolution of the gauge-invariant phase difference $\varphi = \theta_2 - \theta_1 - \frac{2\pi}{\Phi_0} \int \mathbf{A} \cdot d\mathbf{s}$ between adjacent islands. Here Φ_0 is the magnetic flux quantum and $\mathbf{A}$ is the vector potential of the external magnetic field (integration goes from one island to the other one). In the following, we consider zero magnetic fields $\mathbf{A} = \mathbf{0}$. The mechanical analog of a biased Josephson junction is a damped pendulum driven by a constant torque. There are two general states in this system: the first state corresponds to a stable equilibrium, and the second one corresponds to a whirling pendulum state. When treated for a chain of coupled pendula, the DB corresponds to the whirling state of a few adjacent pendula with all other pendula performing oscillations around their stable equilibria. In an array of Josephson junctions the nature of the coupling between the junctions is inductive. A localized excitation in such a system corresponds to a state where one (or several) junctions are in the whirling (resistive) state, with all other junctions performing small forced oscillations around their stable equilibria. According to theoretical predictions [11], the amplitude of these oscillations should decrease exponentially with increasing distance from the center of the excitation.

We have conducted experiments with ladders consisting of Nb/Al-AlO_x/Nb underdamped Josephson tunnel junctions [12]. We investigated annular ladders (closed in a ring) as well as straight ladders with open boundaries. The sketch of an annular ladder is given in Fig. 1. Each cell contains 4 small Josephson junctions. The size of the hole between the superconducting electrodes which form the cell is about $3 \times 3\ \mu\text{m}^2$. Here we define *vertical* junctions (JJ_V) as those in the direction of the external bias current, and *horizontal* junctions (JJ_H) as those transverse to the bias. Because of fabrication reasons we made the superconducting electrodes quite broad so that the distance between two neighboring vertical junctions is 30 μm, as can be seen in Fig. 3. The ladder voltage is read across the vertical junctions. According to the Josephson relation, a junction in a whirling state generates a dc voltage

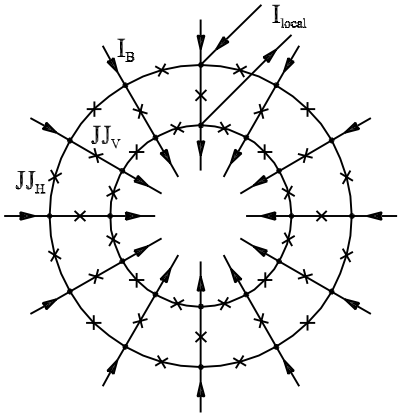

FIG. 1. Schematic view of an annular ladder. Josephson junctions are indicated by crosses (×).

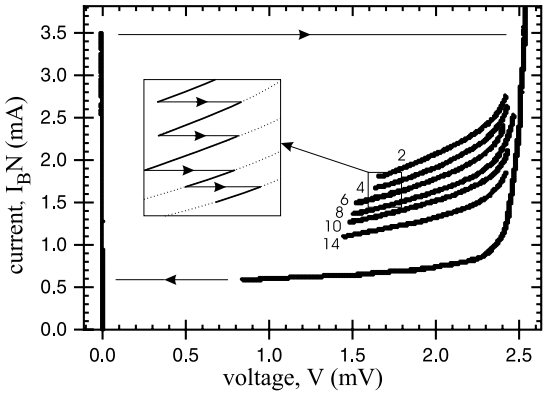

FIG. 2. Current-voltage I_B-V plane for an annular ladder with the parameters $N = 30$, $\eta = 0.44$, and $\beta_L = 2.7$. Digits indicate the number of rotating vertical junctions.

$V = \frac{1}{2\pi}\Phi_0\langle\frac{d\varphi}{dt}\rangle$, where $\langle\cdots\rangle$ means the time average. In order to force junctions into the whirling state we used two different types of bias. The current I_B was uniformly injected at every node via thin-film resistors. Another current I_{local} was applied locally across just one vertical junction.

We studied ladders with different strengths of horizontal and vertical Josephson coupling determined by the junction areas. The ratio of the junction areas is called the anisotropy factor and is expressed in terms of the junction critical currents $\eta = I_{cH}/I_{cV}$. If this factor is equal to zero, vertical junctions will be decoupled and can operate independently one from another. Measurements have been performed at 4.2 K. The number of cells N in different ladders varied from 10 to 30. The discreteness of the ladder is expressed in terms of the parameter $\beta_L = 2\pi LI_{cV}/\Phi_0$, where L is the self-inductance of the elementary cell of the ladder. The damping coefficient $\alpha = \sqrt{\Phi_0/(2\pi I_c CR_N^2)}$ is the same for all junctions as their capacitance C and resistance R_N scale with the area and $C_H/C_V = R_{NV}/R_{NH} = \eta$. The damping α in the experiment can be controlled by temperature and its typical values are between 0.1 and 0.02.

We have measured the dc voltage across various vertical junctions as a function of the currents I_{local} and I_B. In order to generate a localized rotating state in a ladder we started with applying the local current $I_{local} > 2I_{cH} + I_{cV}$. This switches one vertical and the nearest horizontal junctions into the resistive state. After that I_{local} was reduced and, simultaneously, the homogeneous bias I_B was tuned up. In the final state we kept the bias I_B constant and reduced I_{local} to zero. Under these conditions, with a *spatially homogeneous* bias injection, we observed a *spatially localized* rotating state with nonzero dc voltage drops on just one or a few vertical junctions.

Various measured states of the annular ladder in the current-voltage I_B-V plane with $I_{local} = 0$ are presented in Fig. 2. The voltage V is recorded locally on the same vertical junction which was initially excited by the local current injection. The vertical line on the left side corresponds to the superconducting (static) state. The rightmost (also the bottom) curve accounts for the spatially homogeneous whirling state (all vertical junctions rotate synchronously). Its nonlinear $I_B(V)$ shape is caused by a strong increase of the normal tunneling current at a voltage of about 2.5 mV corresponding to the superconducting energy gap. The series of branches represent various localized states. These states differ from each other by the number of rotating vertical junctions.

In order to visualize various rotating states in our ladders we used the method of low temperature scanning laser microscopy [13]. It is based on the mapping of a sample voltage response as a function of the position of a focused low-power laser beam on its surface. The laser beam locally heats the sample and, therefore, introduces an additional dissipation in the area of a few micrometers in diameter. Such a dissipative spot is scanned over the sample and the voltage variation at a given bias current is recorded as a function of the beam coordinate. The resistive junctions of the ladder contribute to the voltage response, while the junctions in the superconducting state show no response. The power of the laser beam is modulated at a frequency of several kHz and the sample voltage response is measured using a lock-in technique.

Several examples of the ladder response are shown in Fig. 3 as 2D gray scale maps. The spatially homogeneous whirling state is shown in Fig. 3(A). Here all vertical junctions are rotating, but the horizontal ones are not. Figure 3(B) corresponds to the uppermost branch of Fig. 2. We observe a localized whirling state expected for a DB, namely a rotobreather [10]. In this case 2 vertical junctions and 4 horizontal junctions of the DB are rotating, with all others remaining in the superconducting state. The same state is shown on an enlarged scale in Fig. 3(C). Figure 3(D) illustrates another rotobreather found for the next lower branch of Fig. 2 at which 4 vertical junctions are in the resistive state. The local current at the beginning of each experiment is passing through the vertical junction being the top one on each map. In Fig. 3(E), which

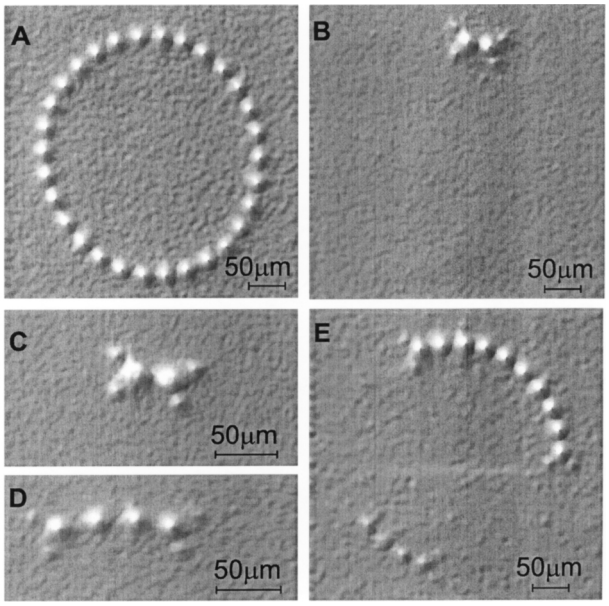

FIG. 3. Whirling states measured in the annular ladder using the low temperature scanning laser microscope: (A) spatially homogeneous whirling state, (B)–(E) various localized states corresponding to discrete breathers.

accounts for one of the lowest branches, we find an even broader localized state. Simultaneously, on the opposite side of the ring we observe another DB excited spontaneously (without any local current). An interesting fact is that in experiments with open boundary ladders (not closed in a ring) we also detected DBs with even or odd numbers of whirling vertical junctions.

Various states shown in Fig. 3 account for different branches in the I_B-V plane in Fig. 2. Each resistive configuration is found to be stable along its particular branch. On a given branch the damping of the junctions in the rotating state is compensated by the driving force of the bias current I_B. The transitions between the branches are discontinuous in voltage. In Fig. 2, we see that all branches of localized states lose their stability at a voltage of about 1.4 mV. Furthermore, as indicated in the inset on Fig. 2, a peculiar switching occurs: upon *lowering* the bias current I_B the system switches to a *larger* voltage. According to our laser microscope observations, the lower the branch in Fig. 2, the larger the number M of resistive vertical junctions. The slope of these branches is $dV/dI_B \approx MR_{NV}/(M + \eta)$, thus the branches become very close to each other for large M. The fact that the voltage at the onset of instability is independent of the size of the DB, indicates that the instability is essentially local in space and occurs at the border between the resistive and nonresistive junctions.

The occurrence of DBs is inherent to our system. We have also found various localized states to arise without any local current. Namely, when biasing the ladder by the homogeneous current I_B slightly below NI_{cV}, we sometimes observed the system switching to a spatially inhomogeneous state, similar to that shown in Fig. 3(E).

To interpret the experimental observations, we analyze the equations of motion for our ladders (see [11] for details). Denote by $\varphi_l^v, \varphi_l^h, \tilde{\varphi}_l^h$ the phase differences across the lth vertical junction and its right upper and lower horizontal neighbors. Using $\nabla\varphi_l = \varphi_{l+1} - \varphi_l$ and $\Delta\varphi_l = \varphi_{l+1} + \varphi_{l-1} - 2\varphi_l$, the Josephson equations yield

$$\ddot{\varphi}_l^v + \alpha\dot{\varphi}_l^v + \sin\varphi_l^v = \gamma - \frac{1}{\beta_L}(-\Delta\varphi_l^v + \nabla\tilde{\varphi}_{l-1}^h - \nabla\varphi_{l-1}^h), \quad (1)$$

$$\ddot{\varphi}_l^h + \alpha\dot{\varphi}_l^h + \sin\varphi_l^h = -\frac{1}{\eta\beta_L}(\varphi_l^h - \tilde{\varphi}_l^h + \nabla\varphi_l^v), \quad (2)$$

$$\ddot{\tilde{\varphi}}_l^h + \alpha\dot{\tilde{\varphi}}_l^h + \sin\tilde{\varphi}_l^h = \frac{1}{\eta\beta_L}(\varphi_l^h - \tilde{\varphi}_l^h + \nabla\varphi_l^v). \quad (3)$$

Here $\gamma = I_B/(NI_{cV})$. First, we compute the dispersion relation for Josephson plasmons $\varphi \propto e^{i(ql-\omega t)}$ at $\alpha = 0$ in the ground state (no resistive junctions). We obtain three branches: one degenerated with $\omega = 1$ (horizontal junctions excited in phase), the second one below $\omega = 1$ with weak dispersion (mainly vertical junctions excited), and finally the third branch with the strongest dispersion above the first two branches (mainly horizontal junctions excited out of phase), cf. the inset in Fig. 4. The region of experimentally observed DB stability is also shown. Note, that for DBs with symmetry between the upper and lower horizontal junctions the voltage drop on the horizontal junctions is half the drop across the vertical ones. This causes the characteristic frequency of the DB to be 2 times smaller than the value expected from the measured voltage drop on the vertical junctions [11].

In order to compare experimental results of Fig. 2 to the model given by Eqs. (1)–(3), we have integrated the latter equations numerically. We also find localized DB solutions, in particular solutions similar to the ones reported in previous numerical studies [11]. These solutions are generated with using initial conditions when M vertical junctions of the resistive cluster (cf. Fig. 3) have $\varphi = 0$ and $\dot{\varphi} = 2V_0$ and the horizontal junctions adjacent to the vertical resistive cluster have $\varphi = 0$ and $\dot{\varphi} = V_0$, while all other phase space variables are set to zero. The obtained I_B-V curves are shown in Fig. 4. The superconducting gap structure and the nonlinearity of slopes are not reproduced in the simulations, as we use a voltage independent dissipation constant α in (1)–(3). We find several instability windows of DB solutions, separating stable parts of the I_B-V characteristics.

In addition to direct numerical calculation of I_B-V curves, we have also computed numerically exact DB solutions of (1)–(3) by using a generalized Newton map [1]. We have studied the linear stability of the obtained DB [1] by solving the associated eigenvalue problem. The spatial profile of the eigenmode which drives the

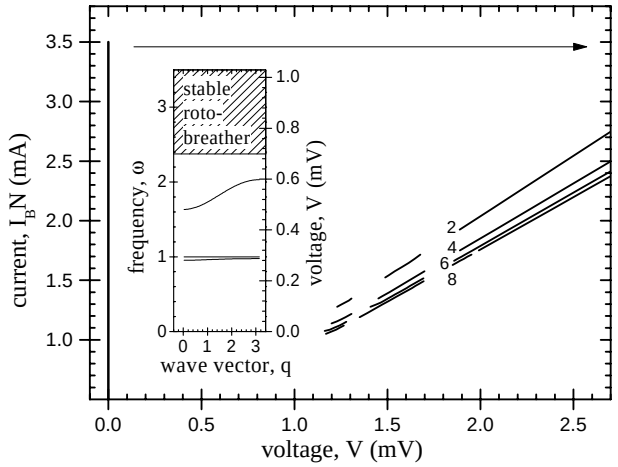

FIG. 4. I_B-V characteristics for numerically obtained breather states with 2, 4, 6, and 8 whirling vertical junctions. The inset shows the dispersion relation of an annular ladder with $\gamma = 0.3$, $\alpha = 0.07$, $N = 30$, $\eta = 0.44$, and $\beta_L = 2.7$.

instability (associated with the edges of the instability windows in Fig. 4) is localized on the DB, more precisely on the edges of the resistive domain. This is in accord with the experimental observation (Fig. 3) where several independent DBs can be excited in the system.

The DB states turn to be either invariant under $\varphi_l^h \leftrightarrow \tilde{\varphi}_l^h$ transformation or not. Both such solutions have been obtained numerically. To understand this, we consider the equations of motion (1)–(3) in the limit $\eta \to 0$ and look for time-periodic localized solutions. In this limit the brackets on the right-hand side of (2) and (3) vanish, and vertical junctions decouple from each other. Let us then choose one vertical junction with $l = 0$ to be in a resistive state and all the others to be in the superconducting state. To satisfy periodicity in the horizontal junction dynamics we arrive at the condition

$$\varphi_0^h = \frac{1}{k}\varphi_0^v, \qquad \tilde{\varphi}_0^h = -\frac{k-1}{k}\varphi_0^v$$

or

$$\varphi_0^h = \frac{k-1}{k}\,\varphi_0^v, \qquad \tilde{\varphi}_0^h = -\frac{1}{k}\,\varphi_0^v \tag{4}$$

and a similar set of choices for $\varphi_{-1}^h, \tilde{\varphi}_{-1}^h$, with all other horizontal phase differences set to zero. Here k is an arbitrary positive integer. Continuation to nonzero η values should be possible [6]. The symmetric DBs in Fig. 3 correspond to $k = 2$. The mentioned asymmetric DBs correspond to $k = 1$. The current-voltage characteristics for asymmetric $k = 1$ DBs show a different behavior from that discussed above. These DBs are stable down to very small current values, and simply disappear upon further lowering of the current, so that the system switches from a state with finite voltage drop to a pure superconducting state with zero voltage drop.

The observed DB states are clearly different for the well-known row switching effect in 2D Josephson junction arrays. The DBs demonstrate localization transverse to the bias current (driving force), whereas the switched states of *noninteracting junction rows* are localized along the current. At the same time, DB states inherent to Josephson ladders are closely linked to the recently discovered meandering effect in 2D arrays [14].

In summary, we have experimentally detected various types of rotobreathers in Josephson ladders and visualized them with the help of laser microscopy. Our experiments show that DBs in Josephson ladders may occupy several lattice sites and that the number of occupied sites may increase at specific instability points. The possibility of exciting DBs spontaneously, without using any local force, demonstrates their inherent character. The observed DBs are stable in a wide frequency range. Numerical calculations confirm the reported interpretation and allow for a detailed study of the observed instabilities.

Note added.—After this work was completed we became aware of the experiment [15] which detected 1- and 2-site rotobreathers by using several voltage probes across a ladder. We note that our method allows for direct visual observation of any multisite breathers.

[1] S. Flach and C. R. Willis, Phys. Rep. **295**, 181 (1998).
[2] S. Aubry, Physica (Amsterdam) **103D**, 201 (1997).
[3] A. A. Ovchinnikov and H. S. Erikhman, Usp. Fiz. Nauk **138**, 289 (1982).
[4] S. Takeno, M. Kubota, and K. Kawasaki, Physica (Amsterdam) **113D**, 366 (1998).
[5] R. Lai and A. J. Sievers, Phys. Rep. **314**, 147 (1999).
[6] R. S. MacKay and J. A. Sepulchre, Physica (Amsterdam) **119D**, 148 (1998).
[7] H. S. Eisenberg, Y. Silberberg, R. Morandotti, A. R. Boyd, and J. S. Aitchison, Phys. Rev. Lett. **81**, 3383 (1998).
[8] B. I. Swanson, J. A. Brozik, S. P. Love, G. F. Strouse, A. P. Shreve, A. R. Bishop, W.-Z. Wang, and M. I. Salkola, Phys. Rev. Lett. **82**, 3288 (1999).
[9] U. T. Schwarz, L. Q. English, and A. J. Sievers, Phys. Rev. Lett. **83**, 223 (1999).
[10] L. M. Floria, J. L. Marin, P. J. Martinez, F. Falo, and S. Aubry, Europhys. Lett. **36**, 539 (1996).
[11] S. Flach and M. Spicci, J. Phys. Condens. Matter **11**, 321 (1999).
[12] HYPRES Inc., Elmsford, NY 10523.
[13] A. G. Sivakov, A. P. Zhuravel', O. G. Turutanov, and I. M. Dmitrenko, Appl. Surf. Sci. **106**, 390 (1996).
[14] D. Abraimov, P. Caputo, G. Filatrella, M. V. Fistul, G. Yu. Logvenov, and A. V. Ustinov, Phys. Rev. Lett. **83**, 5354 (1999).
[15] E. Trias, J. J. Mazo, and T. P. Orlando preceding Letter, Phys. Rev. Lett. **84**, 741 (2000).

Diversity of discrete breathers observed in a Josephson ladder

P. Binder, D. Abraimov, and A. V. Ustinov
Physikalisches Institut III, Universität Erlangen-Nürnberg, Erwin-Rommel-Straße 1, D-91058 Erlangen, Germany
(Received 28 February 2000)

We generate and observe discrete rotobreathers in Josephson junction ladders with open boundaries. Rotobreathers are localized excitations that persist under the action of a spatially uniform force. We find a rich variety of stable dynamic states including pure symmetric, pure asymmetric, and mixed states. The parameter range where the discrete breathers are observed in our experiment is limited by retrapping due to dissipation.

PACS number(s): 05.45.Yv, 63.20.Ry, 74.50.+r

Nonlinearity and lattice discreteness lead to a generic class of excitations that are spatially localized on a scale comparable to the lattice constant. These excitations, also known as *discrete breathers*, have recently attracted much interest in the theory of nonlinear lattices [1–3]. It is believed that discrete breathers might play an important role in the dynamics of various physical systems consisting of coupled nonlinear oscillators. It has even been said that for discrete nonlinear systems breathers might be as important as are solitons for continuous nonlinear media.

There have been several recent experiments that reported on generation and detection of discrete breathers in diverse systems. These are low-dimensional crystals [4], antiferromagnetic materials [5], coupled optical waveguides [6], and Josephson junction arrays [7,8]. By using the method of low-temperature scanning laser microscopy, we have recently reported direct visualization of discrete breathers [8]. In this paper we present measurements of localized modes in Josephson ladders. Using the same method as in our first experiment, we study an even more tightly coupled lattice of Josephson junctions and observe a rich diversity of localized excitations that persist under the action of a spatially uniform force.

A biased Josephson junction behaves very similarly to its mechanical analog, which is a forced and damped pendulum. An electric bias current flowing across the junction is analogous to a torque applied to the pendulum. The maximum torque that the pendulum can sustain and remain static corresponds to the critical current I_c of the junction. For low damping and bias below I_c, the junction allows for two states: the superconducting (static) state and the resistive (rotating) state. The phase difference φ of the macroscopic wave functions of the superconducting islands on both sides of the junction plays the role of the angle coordinate of the pendulum. According to the Josephson relation, a junction in a rotating state generates dc voltage $V=(1/2\pi)\Phi_0\langle d\varphi/dt\rangle$, where $\langle\cdots\rangle$ is the time average. By connecting many Josephson junctions with superconducting leads one gets an array of coupled nonlinear oscillators.

We perform experiments with a particular type of Josephson junction array called the Josephson ladder. Theoretical studies [9–11] of these systems have predicted the existence of spatially localized excitations called rotobreathers. Rotobreathers are 2π-periodic solutions in time that are exponentially localized in space.

Measurements are performed on linear ladders (with open boundaries) consisting of Nb/Al-AlO_x/Nb underdamped Josephson tunnel junctions [12]. An optical image [Fig. 1(a)] shows a linear ladder that is schematically sketched in Fig. 1(b). Each cell contains four small Josephson junctions. The size of the hole between the superconducting electrodes that form the cell is about 3×3 μm^2. The distance between the Josephson junctions is about 24 μm. The number of cells N in the ladder is 10. Measurements presented in this paper have been performed at 5.2 K. The bias current I_B was uniformly injected at every node via thin-film resistors $R_B=32$ Ω. Here we define *vertical* junctions (JJ_V) as those in the direction of the external bias current, and *horizontal* junctions (JJ_H) as those transverse to the bias. The ladder voltage was read across the central vertical junction. The damping coefficient $\alpha=\sqrt{\Phi_0/(2\pi I_c C R_{sg}^2)}$ is the same for all junctions as their capacitance C and subgap resistance R_{sg} scale

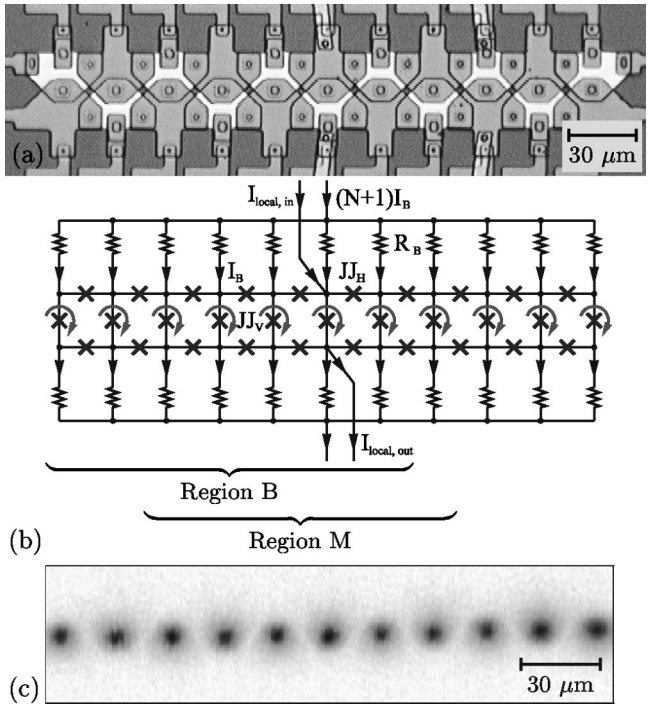

FIG. 1. Optical (a) and schematic (b) view of a linear ladder. (c) Spatially homogeneous whirling state measured by the laser scanning technique.

with the area and $C_H/C_V=R_{sgV}/R_{sgH}$. The damping α in the experiment can be controlled by temperature and its typical values vary between 0.1 and 0.02.

There are two types of coupling between cells in a ladder. The first is the inductive coupling between the cells that is expressed by the self-inductance parameter $\beta_L=2\pi LI_{cV}/\Phi_0$, where L is the self-inductance of the elementary cell. The second is the nonlinear Josephson coupling via horizontal junctions. The ratio of the horizontal and vertical junction areas is called the anisotropy factor and can be expressed in terms of the junction critical currents $\eta=I_{cH}/I_{cV}$. If this factor is equal to zero, the vertical junctions are decoupled and operate independently from one another. On the other hand, if this factor goes to infinity the ladder behaves like a parallel one-dimensional array and no rotobreather can exist since no magnetic flux can enter through the horizontal junctions. Thus, it is an important challenge to increase the anisotropy as far as possible. In this work we present measurements for the highest anisotropy factor ($\eta=0.56$) studied up to now to our knowledge. In contradiction to the existing theoretical prediction [11] for this anisotropy value, in the studied parameter range with moderate dissipation we find a rich diversity of localized excitations.

To briefly introduce the role of the parameters we quote the equations of motion for our system (see Ref. [10] for details):

$$\ddot{\varphi}_l^V+\alpha\dot{\varphi}_l^V+\sin\varphi_l^V=\gamma-\frac{1}{\beta_L}(-\Delta\varphi_l^V+\nabla\tilde{\varphi}_{l-1}^H-\nabla\varphi_{l-1}^H), \tag{1}$$

$$\ddot{\varphi}_l^H+\alpha\dot{\varphi}_l^H+\sin\varphi_l^H=-\frac{1}{\eta\beta_L}(\varphi_l^H-\tilde{\varphi}_l^H+\nabla\varphi_l^V), \tag{2}$$

$$\ddot{\tilde{\varphi}}_l^H+\alpha\dot{\tilde{\varphi}}_l^H+\sin\tilde{\varphi}_l^H=\frac{1}{\eta\beta_L}(\varphi_l^H-\tilde{\varphi}_l^H+\nabla\varphi_l^V), \tag{3}$$

where φ_l^V,φ_l^H, and $\tilde{\varphi}_l^H$ are the phase differences across the lth vertical junction and its right upper and lower horizontal neighbors, $\nabla\varphi_l=\varphi_{l+1}-\varphi_l$, $\Delta\varphi_l=\varphi_{l+1}+\varphi_{l-1}-2\varphi_l$, and $\gamma=I_B/I_{cV}$ is the normalized bias current.

In order to generate a discrete breather in a ladder we used the technique described in Ref. [8]. We used two extra bias leads for the middle vertical Josephson junction [cf.Fig. 1(b)] to apply a local current $I_{local}>I_{cV}$. This current switches the vertical junction into the resistive state. At the same time, forced by magnetic flux conservation, one or two horizontal junctions on both sides of the vertical junction also switch to the resistive state. After that I_{local} is reduced and, simultaneously, the uniform bias I_B is tuned up. In the final state, we keep the bias I_B smaller than I_{cV} and have reduced I_{local} to *zero*. By changing the starting value of I_{local} it is possible to get more than one vertical junction rotating. When trying the slightly different current sweep sequence described in Ref. [7] we generated mainly states with many rotating vertical junctions.

In all measurements presented below, we have measured the dc voltage across the middle vertical junction as a function of the homogeneous bias current I_B. We used the method of low-temperature scanning laser microscopy [13] to obtain electrical images from the dynamic states of the ladder. The laser beam locally heats the sample and changes the dissipation in an area of several micrometers in diameter. If the junction at the heated spot is in the resistive state, a voltage change will be measured. By scanning the laser beam over the whole ladder we can visualize the rotating junctions.

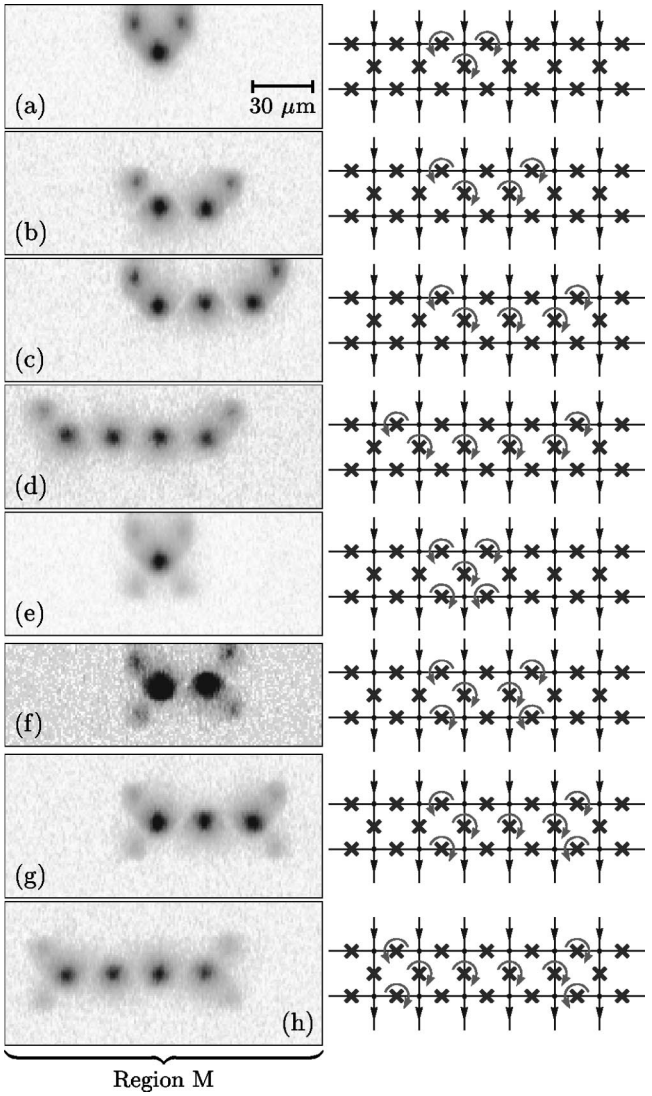

FIG. 2. Various localized states (discrete rotobreathers) measured by the low-temperature scanning laser microscope: (a)–(d) asymmetric rotobreathers; (e)–(h) symmetric rotobreathers. Region *M* is illustrated in Fig. 1(b).

Various measured ladder states are shown in Fig. 2 as two-dimensional gray scale maps. The gray scale corresponds to the measured voltage response during the laser scanning. In Fig. 2(a) we present the simplest of observed states, an *asymmetric* single-site rotobreather, where one vertical Josephson junction and the upper adjacent horizontal Josephson junctions are in the resistive state. On the right side of the plot we show the corresponding schematic view with arrows marking the rotating junctions. In the case of Fig. 2(b) two vertical junctions and two horizontal junctions are rotating that corresponds to an asymmetric two-site breather. An asymmetric three-site breather and an asymmet-

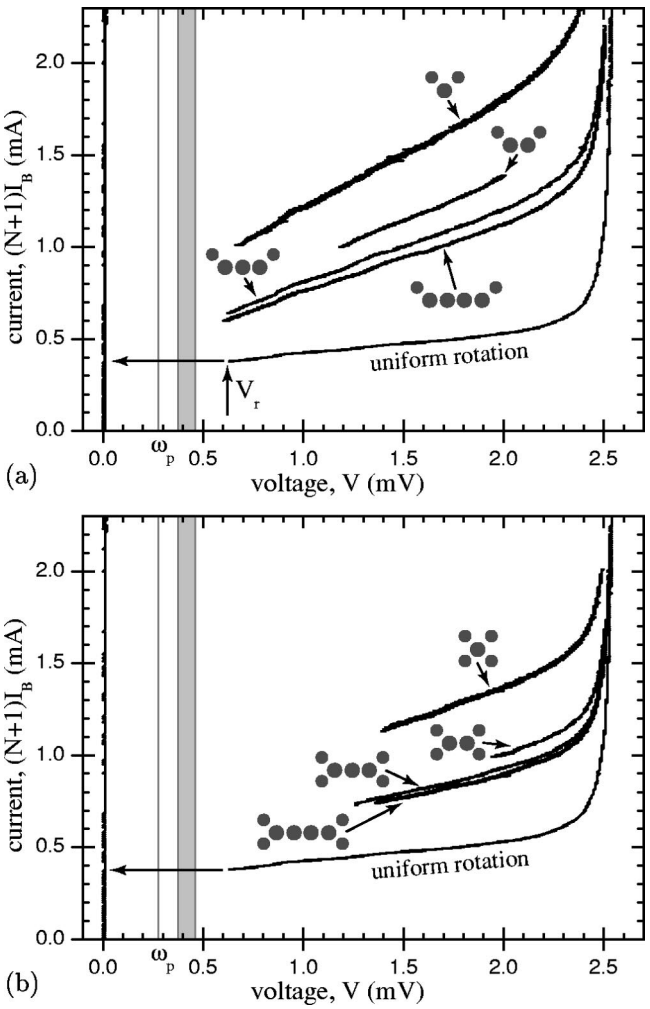

FIG. 3. I_B-V characteristics for asymmetric (a) and symmetric (b) breathers in a ladder with the parameters $N=10$, $I_{cV}=320$ μA, $\eta=0.56$, and $\beta_L=4.3$. The gray region indicates the frequency range of the upper plasmon band. ω_p is the plasma frequency.

ric four-site breather are shown in Figs. 2(c) and 2(d), respectively. Here, the voltages of the whirling horizontal and vertical junctions are equal due to magnetic flux conservation. The magnetic flux enters the ladder through one horizontal junction, goes through the vertical ones, and leaves the ladder through another horizontal junction. When a single magnetic flux quantum passes through a Josephson junction its phase φ changes by 2π. In contrast to our previous measurements of an annular ladder [8], here in ladders with open boundaries we observe asymmetric breathers as frequently as symmetric breathers. The I_B-V characteristics of these localized states are presented in Fig. 3(a). Particular states indicated on the plot are stable along the measured curves. The more junctions are whirling, the higher is the measured resistance.

Another type of discrete breather observed in our experiment is shown in Figs. 2(e)–(h). Figure 2(e) illustrates a *symmetric* single-site breather with one vertical and all four adjacent horizontal junctions in the resistive state. Though we call this state symmetric, the upper and lower horizontal junctions may in general have different voltages. The simplest voltage-symmetric case would be when each horizontal junction voltage is equal to half of the voltage of the whirling vertical junction [8]. We also observed a variety of multisite breathers of this type. A two-site, a three-site, and a four-site breather are shown in Figs. 2(f), 2(g), and 2(h), respectively. The corresponding I_B-V characteristics over the stability range of symmetric breathers are presented in Fig. 3(b).

As mentioned above, Figs. 3(a) and 3(b) show the I_B-V characteristics with $I_{local}=0$ of asymmetric and symmetric rotobreathers, respectively. The voltage V is always recorded locally on the middle vertical junction, which was initially excited by the local current injection. The vertical line on the left side corresponds to the superconducting (static) state. The rightmost (also the bottom) curve accounts for the spatially uniform whirling state (all vertical junctions rotate synchronously and horizontal junctions are not rotating). An electrical image of this state is shown in Fig. 1(c). The upper branches in Fig. 3 represent various localized states. The uppermost branch corresponds to a single-site breather, the next lower branch to a two-site breather, and so on.

It is easy to show that the voltage V_r at which the vertical and horizontal junctions switch back to the superconducting state is the same. By using $R_{sgV}/R_{sgH}=\eta$ and $I_{cH}/I_{cV}=\eta$ we get with $I_r \propto I_c$ that $V_r=R_{sgV}I_{rV}=R_{sgH}I_{rH}$. For the uniform state we observed $V_r \approx 0.6$ mV. At about the same voltage, the whirling horizontal and vertical junctions for the asymmetric breather are retrapped to the static state as can be seen in Fig. 3(a). The symmetric breathers show different behavior. Assuming $V_H \approx V_V/2$, we can expect that at the voltage $V=2V_r \approx 1.2$ mV the horizontal junctions should already be trapped into the superconducting state. But if the voltages of the top and bottom horizontal junctions are not equal while I_B is decreased, the retrapping current in the junction with the lower voltage is reached earlier and the retrapping occurs at a higher measured voltage.

We found that in order to explain the retrapping current of the breather states the bias resistors R_B have to be taken into account. Initially, these resistors were designed to provide a uniform bias current distribution in the ladder. Assuming that the Josephson junctions in the superconducting state are just short circuits, we get the electric circuits that are shown as insets in Fig. 4. The total current injected in the breather region is calculated by using the resistance R of vertical junctions measured in the spatially uniform state. Thus we derive the retrapping current as

$$(N+1)I_B=\left[\frac{(N-M+1)}{(1+\delta)R_B}+\frac{(N+1)[M+(2-\delta)\eta]}{MR}\right]V, \tag{4}$$

where M is the number of whirling vertical junctions. The parameter δ is equal to 0 for asymmetric breathers and to 1 for symmetric breathers. The calculated retrapping current is compared with the experiment in Fig. 4. For the asymmetric breathers the agreement is fairly good. We believe that the larger discrepancy for the symmetric breathers is due to the assumption $V_H=V_V/2$ that we imposed in the derivation of the retrapping current.

One interesting feature in our experiment is the dynamical behavior of the local states in the linear ladder, which differs from the previous observations in the annular ladder [8] with the anisotropy parameter $\eta=0.44$. In Fig. 5 this feature is illustrated for three-site breathers. After the creation of a

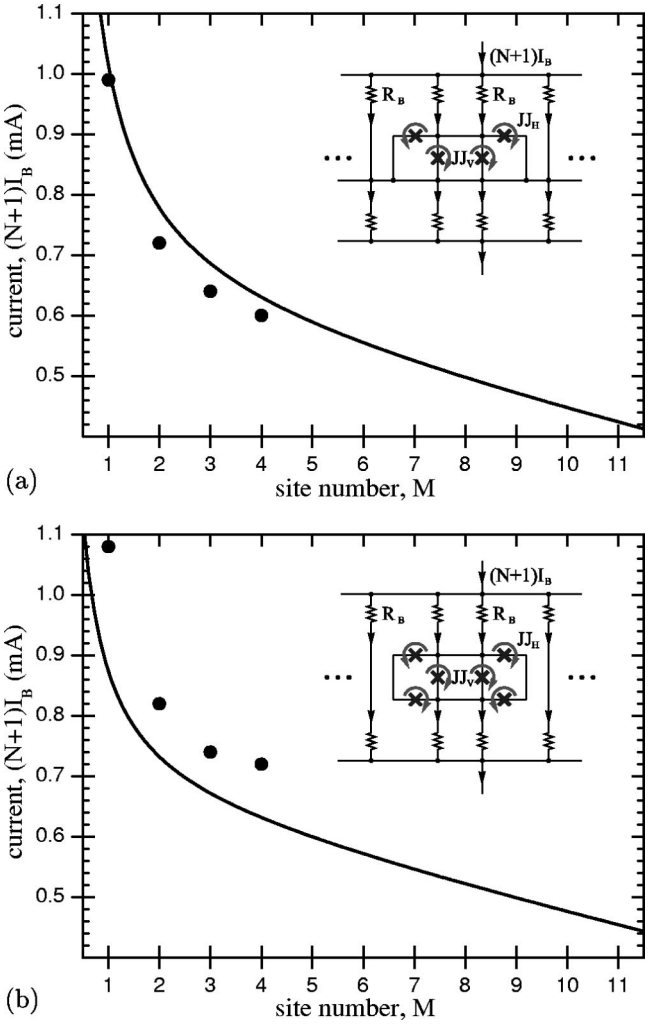

FIG. 4. The retrapping current measured (points) and calculated (line) by Eq. (4) for the asymmetric (a) ($V=V_r$) and the symmetric (b) ($V=2V_r$) rotobreathers. The insets show the reduced electric circuits for each case.

symmetric rotobreather (middle curve) we lower the uniform bias current I_B until the retrapping current of one of the horizontal junctions at each side is reached. Here we observe switching to the corresponding asymmetric three-site rotobreather state. By further lowering of the bias current we get to the point where both the vertical and the horizontal junctions reach their retrapping currents and the whole ladder goes into the superconducting state. If, instead of lowering the bias current, we start increasing it, another switching point is observed where the previous symmetric breather state is recovered. In contrast to this behavior, in the annular ladder [8] the observed lower instability of the symmetric breather led to an *increase* of voltage [14].

In addition to the simplest hierarchic states described above we also found a large variety of more complex localized dynamic states. Some examples are presented in Fig. 6. Figures 6(a)–6(c) are sections from the middle region (M) [cf. Fig. 1(b)] of the measured linear ladder. Figure 6(a) shows an asymmetric six-site breather with top and bottom horizontal junctions whirling on its sides. Figure 6(b) illustrates a three-site rotobreather that is symmetric on one side and asymmetric on the other. Another very peculiar localized

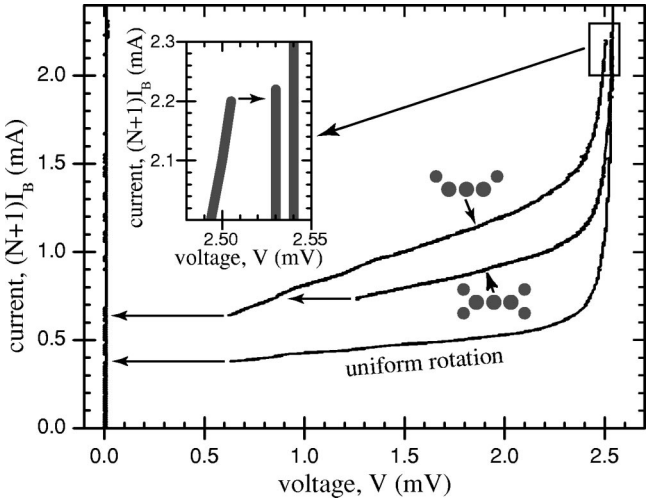

FIG. 5. I_B-V characteristics of three-site breathers.

state is presented in Fig. 6(c). The rightmost vertical junction is rotating with a lower frequency than the other four vertical junctions on the left. This can be understood from the appearance of an extra rotating horizontal junction in the interior of this state. We can interpret it as a four-site breather coupled to a single-site breather. All these localized states would be topologically forbidden in the case of an annular ladder, as the magnetic flux inside the superconducting circuit should not accumulate, but they are not forbidden in a ladder with open boundaries. The last two pictures 6(d) and 6(e) are taken near the border of the ladder. We find here truncated asymmetric and symmetric six-site breathers. The marginal vertical junction does not require any horizontal junctions to rotate.

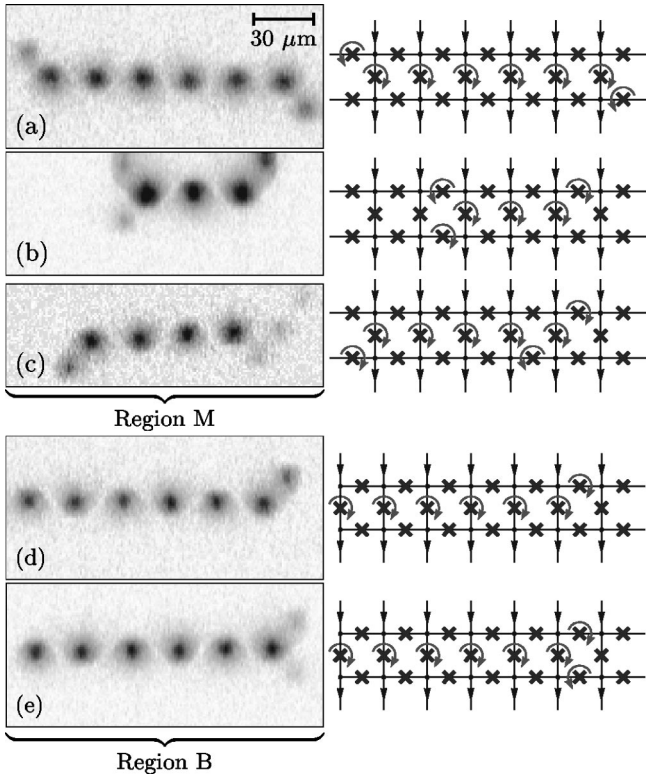

FIG. 6. More complex nonuniform states measured in the middle (M) and on the border (B) regions of the ladder.

In summary, we have presented observations of a large variety of spatially localized dynamic rotobreather states in Josephson ladders with open boundaries. These states can be excited by local current injection and supported by a uniform current bias. We observe both the symmetric and asymmetric rotobreather states predicted in Ref. [11], as well as more complex mixed states. We believe that the region of existence and stability of rotobreathers depends sensitively on dissipation, discreteness, and the anisotropy parameter of the ladder.

This work was supported by EC Contract No. HPRN-CT-1999-00163 and the Deutsche Forschungsgemeinschaft (DFG). We would like to thank S. Aubry, A. Brinkman, S. Flach, R. Giles, Yu. S. Kivshar, and Y. Zolotaryuk for stimulating discussions.

[1] S. Takeno and M. Peyrard, Physica D **92**, 140 (1996).
[2] S. Aubry, Physica D **103**, 201 (1997).
[3] S. Flach and C.R. Willis, Phys. Rep. **295**, 181 (1998).
[4] B.I. Swanson, J.A. Brozik, S.P. Love, G.F. Strouse, A.P. Shreve, A.R. Bishop, W.-Z. Wang, and M.I. Salkola, Phys. Rev. Lett. **82**, 3288 (1999).
[5] U.T. Schwarz, L.Q. English, and A.J. Sievers, Phys. Rev. Lett. **83**, 223 (1999).
[6] H.S. Eisenberg, Y. Silberberg, R. Morandotti, A.R. Boyd, and J.S. Aitchison, Phys. Rev. Lett. **81**, 3383 (1998).
[7] E. Trías, J.J. Mazo, and T.P. Orlando, Phys. Rev. Lett. **84**, 741 (2000).
[8] P. Binder, D. Abraimov, A.V. Ustinov, S. Flach, and Y. Zolotaryuk, Phys. Rev. Lett. **84**, 745 (2000).
[9] L.M. Floría, J.L. Marin, P.J. Martinez, F. Falo, and S. Aubry, Europhys. Lett. **36**, 539 (1996).
[10] S. Flach and M. Spicci, J. Phys.: Condens. Matter **11**, 321 (1999).
[11] J.J. Mazo, E. Trías, and T.P. Orlando, Phys. Rev. B **59**, 13 604 (1999).
[12] HYPRES Inc., Elmsford, NY 10523.
[13] A.G. Sivakov, A.P. Zhuravel', O.G. Turutanov, and I.M. Dmitrenko, Appl. Surf. Sci. **106**, 390 (1996).
[14] It should be noted that after completing and publishing (Ref. [8]) our experiments with annular ladders we found out a specific problem in their layout, namely, every second horizontal junction in the inner ring was shorted during fabrication. This explains why mainly breathers with even numbers of rotating vertical junctions were observed.